

Cite this: *Chem. Sci.*, 2019, **10**, 10318

All publication charges for this article have been paid for by the Royal Society of Chemistry

Received 21st August 2019
Accepted 16th September 2019
DOI: 10.1039/c9sc04185k
rsc.li/chemical-science

1. Introduction

Fluorinated compounds have fundamental roles within the pharmaceutical, agrochemical and materials industries.^{1–4} The presence of a fluorine atom imparts profound effects upon the physical, chemical and biological properties of drugs and plant protection agents such as ProzacTM, Lipitor[®], ciprofloxacin and diclosulam.⁵ Such compounds are often synthesised from fluorine-containing building blocks;⁶ a key example is the antifungal agent voriconazole,⁷ which is synthesised from a 5-fluoropyrimidine intermediate that is prepared from a 2-fluoro-1,3-ketoester derivative. In this context, finding selective and efficient routes towards the fluorination of 1,3-dicarbonyl derivatives has been the subject of significant interest. Early work involved fluorinating reagents such as ClO_3F ,⁸ CF_3OF ,⁹ XeF_2 (ref. 10,11) and CsSO_4F ,¹² however, the low selectivities, difficulties regarding preparation, high reactivities and toxicities of these reagents halted their adoption in discovery and manufacturing processes. Elemental fluorine (F_2) has been successfully used for the fluorination of 1,3-dicarbonyl systems, using both batch and flow techniques on laboratory and manufacturing scales, but this reagent requires specialist handling techniques that are not readily available in most laboratories.^{13–18}

With the introduction of shelf-stable, crystalline electrophilic fluorinating reagents of the N–F class, such as SelectfluorTM, NFSI and *N*-fluoropyridinium salts (Fig. 1a), that do not present any handling problems, numerous reports followed regarding the electrophilic fluorination of 1,3-dicarbonyl derivatives. Procedures include catalyst-free reactions,¹⁹ microwave-assisted methods,²⁰ transition metal (Ti and Ru) catalysed methods,^{21–23} solvent-free reactions assisted by milling,^{24,25} fluorinations in ionic liquids,²⁶ and reactions conducted in water.^{27,28} In many cases, difficulties in controlling mono- *versus* difluorination were reported, leading to challenging separations of the product mixtures. Therefore, finding synthetic routes that allow selective fluorination by such widely used reagents would be of great use.

Bioactive compounds bearing CF_2 groups are found in both drugs and agrochemicals (e.g. gemcitabine, pantoprazole, sedaxane).²⁹ In particular, carbonyl and dicarbonyl compounds containing α,α -difluoromethylene moieties are highly desirable bioactive compounds. When adjacent to a carbonyl group, the difluoromethylene moiety greatly increases the electrophilicity of the carbonyl group, leading to very facile nucleophilic additions. These include the additions of nucleophilic residues of enzyme active sites to α,α -difluoroketonic compounds,^{30,31} which have led to the application of α,α -difluoroketones as enzyme inhibitors.^{32–34} For example, difluorostatone compounds have been identified as potent inhibitors of HIV-1 protease³⁵ and of a serine protease in the malaria parasite.³⁶

Despite the importance of organofluorine compounds in the life sciences, very few kinetics studies on fluorination reactions are present in the literature and there have been no quantitative studies on the introduction of two fluorine atoms to form

^aChemistry Department, Durham University, South Road, Durham, DH1 3LE, UK.
E-mail: d.r.w.hodgson@durham.ac.uk

^bAstraZeneca, Pharmaceutical Technology & Development, Macclesfield, SK10 2NA, UK

† Electronic supplementary information (ESI) available. See DOI: [10.1039/c9sc04185k](https://doi.org/10.1039/c9sc04185k)



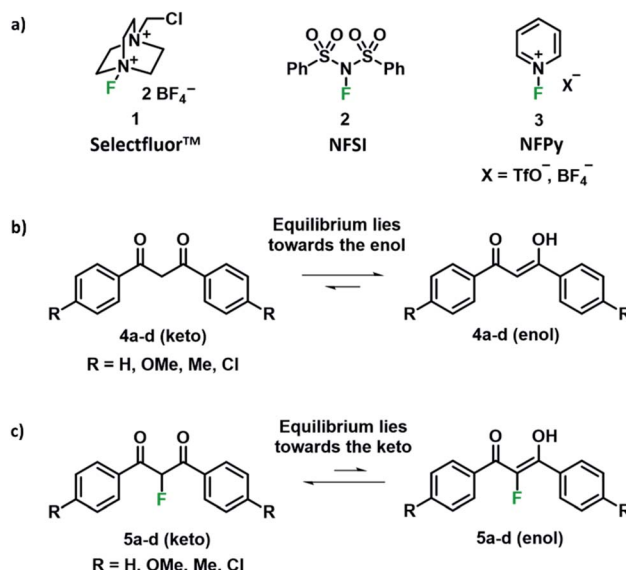


Fig. 1 (a) Commonly used N-F reagents: Selectfluor™, *N*-fluorobenzenesulfonimide (NFSI) and *N*-fluoropyridinium salts (NFPy). (b) Tautomerism in compounds 4a-d. (c) Tautomerism in the fluorine-containing compounds 5a-d.

a difluoromethylene unit. Furthermore, although water and formic acid have been used as solvents or co-solvents in electrophilic fluorination reactions,^{13,28} their effects upon keto–enol tautomerism of 1,3-dicarbonyl derivatives and subsequent fluorinations are not fully understood. We have previously reported a quantitative reactivity scale for electrophilic N-F fluorinating reagents, where absolute and relative rate constants

were determined for the monofluorination of a series of *para*-substituted 1,3-diaryl-1,3-dicarbonyl derivatives by 10 different N-F reagents, in acetonitrile.³⁷ An independent study reported at the same time by Mayr *et al.*³⁸ provided a scale of electrophilicity of the N-F reagents which was in very good agreement. A recent report by Nelson and co-workers³⁹ gave further evidence supporting the S_N2 mechanism for fluorinations by Selectfluor™.

We were intrigued by the keto–enol tautomerism phenomena displayed by our aromatic 1,3-dicarbonyls and their monofluorinated analogues (Fig. 1b and c) and how we could take advantage of their photochemical interconversion properties to study tautomerism and fluorination processes. The mechanism of fluorination proceeds *via* reaction of the enol tautomer with an electrophilic fluorinating reagent,^{14,19} so a full understanding of the factors that affect keto–enol tautomerism would be beneficial in improving selective mono- and difluorinations of 1,3-dicarbonyls. The photochemistry and photophysics of 1,3-diaryl-1,3-dicarbonyl derivatives have been extensively studied.^{40,41} In the 1970s, the groups of Markov^{42,43} and Mazur^{44–46} reported photoisomerization of 1,3-dicarbonyl compounds, whereby the keto–enol equilibrium was perturbed towards the keto tautomer upon irradiation. This process reverses to attain the tautomeric equilibrium by a non-photochemical reaction in darkness. The effects of solvents and additives (ethanol, triethylamine) on the rate of photoketonization were studied by Mazur *et al.*,⁴⁴ however, relaxation kinetics that provided insights into enolization rates were not performed. We therefore identified the photoketonization approach as a means of studying the kinetics of enolization within our nucleophile systems.

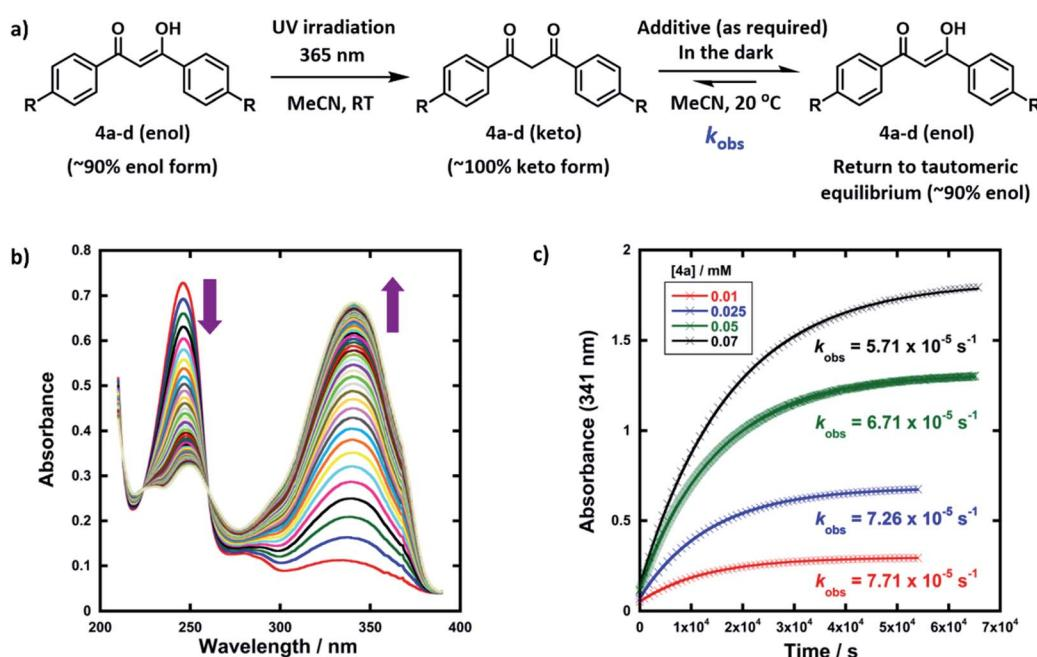


Fig. 2 (a) Reaction scheme for photoketonization (step 1) and relaxation (step 2) of compounds 4a-d in MeCN. (b) Time-arranged multi-wavelength analysis for relaxation of 4a (0.025 mM) in the dark, each spectrum acquired at 15 min intervals at 20 °C. (c) Relaxation of 4a-keto at different concentrations (0.01 mM, 0.025 mM, 0.05 mM and 0.07 mM); k_{obs} values obtained at each concentration of 4a are shown.

Our efforts towards the quantification of the factors which affect mono- *versus* difluorination are two-fold; in the first instance, we focus on the effects of different reaction conditions on the keto-enol tautomerism of the 1,3-diaryl-1,3-dicarbonyl derivatives **4a-d** and **5a-d**. Secondly, we explore and discuss the kinetics of fluorination of enols **4a-d** and fluoroenols **5a-d** and the effects of solvent composition upon these processes.

2. Results and discussion

2.1 Kinetics of keto-enol tautomerism in compounds **4a-d**

The enol forms of 1,3-diaryl-1,3-dicarbonyl derivatives **4a-d** show markedly different absorption spectra to their keto tautomers and are thus convenient systems for the study of tautomerization kinetics by UV-vis spectrophotometry. Compounds **4a-d** were synthesised using previously reported methods,⁴⁷ and they exist predominantly in their enol forms (~90% in MeCN). The enol tautomers were converted to their keto forms by irradiation of solutions of **4a-d** in quartz cuvettes using a 0.5 W UV LED lamp at 365 nm (Fig. 2a). Spectrophotometric monitoring of the photoketonization of each system showed that these processes took several hours (see ESI Section 3.3† for corresponding spectra). The re-equilibration (relaxation) kinetics of **4a-keto** in the dark were monitored using time-arrayed multi-wavelength analysis (Fig. 2b). As relaxation occurred, the enol absorbance band at $\lambda_{\text{max}} = 341$ nm increased while the keto absorbance band at $\lambda_{\text{max}} = 250$ nm decreased. The tautomer equilibrium was regained after ~14 hours, and clean isosbestic points were observed during both the photoketonization and the relaxation processes showing that there was no detectable build-up of additional intermediates during the tautomerization processes on the timescales that we monitored. The re-equilibration of **4a-keto** was studied at four different concentrations and observed first-order rate constants (k_{obs}) were obtained from plots of absorbance at $\lambda_{\text{max}} = 341$ nm over time (Fig. 2c). When the concentration of **4a** was doubled, there was a small decrease in k_{obs} , which could reflect interaction between substrate molecules at higher concentrations.⁴⁸

In order to gain insight into the potential effects of species that are present in widely-employed electrophilic fluorination protocols upon enolization, we explored the effects of water, formic acid, DABCO and $\text{ClCH}_2\text{-DABCO}^+\text{BF}_4^-$ upon re-equilibration kinetics. In addition, because keto-enol equilibration is a reversible process with significant proportions of both keto- and enol-tautomers being present at equilibrium, we also considered the effects of additives upon equilibrium position (K_e). The observed rate constants k_{obs} for re-equilibration of **4a-keto** and the equilibrium constants K_e in the presence of the additives are summarized in Table 1. Forward and reverse rate constants $k_{\text{for}}(\text{H})$ and $k_{\text{rev}}(\text{H})$, respectively, were estimated from k_{obs} values using measured K_e and eqn (1) and (2):

$$k_{\text{obs}} = k_{\text{for}}(\text{H}) + k_{\text{rev}}(\text{H}) \quad (1)$$

$$K_e = k_{\text{for}}(\text{H})/k_{\text{rev}}(\text{H}) \quad (2)$$

Given that the enol forms of **4a-d** are dominant at equilibrium, k_{obs} and $k_{\text{for}}(\text{H})$ values are in the same order. With water as the additive (15–50% of the reaction mixture by volume), increased rates of re-enolization were observed (Fig. 3a), with a 1 : 1 MeCN/water solvent system giving a 10-fold increase in $k_{\text{for}}(\text{H})$ compared to MeCN. The position of the keto-enol equilibrium changed marginally upon moving from MeCN to 1 : 1 MeCN/water, with K_e values of 10.5 and 5.7 respectively. This is consistent with previous studies on 1,3-dicarbonyl systems which show limited variations of K_e values upon changes from single- to mixed-polar solvent systems.⁴⁹ Photophysical studies on di-substituted 1,3-diphenyl-1,3-propanedione compounds have shown that MeCN supports very slow exchange between tautomeric states, whereas protic solvents, including MeCN-water mixtures, enhance rates significantly.^{50,51} Water is often used as a solvent or co-solvent in fluorination reactions to aid solubility of Selectfluor™.²⁸ Our studies show that the solubility limit of Selectfluor™ in water is ~500 mM, compared to ~50 mM in MeCN. Here, we have shown that the addition of water also increases the rate of enolization, facilitating the conversion of the small amounts of residual diketone to the nucleophilic enol tautomer, which reacts with the fluorinating reagent.

The addition of small amounts of formic acid had limited effects on the position of the keto-enol equilibria with all K_e values being ~10, however, greatly enhanced rates of keto-to-enol relaxation were observed (Fig. 3b). Thus, the rate constant for enolization $k_{\text{for}}(\text{H})$ increased 86-fold upon addition of 3% formic acid in comparison to MeCN alone.

The addition of DABCO also increased the relaxation rates significantly. For example, with one equivalent (25 μM), a 330-fold acceleration of the enolization process $k_{\text{for}}(\text{H})$ was observed. Even with 0.1 equivalents (2.5 μM) of DABCO, the tautomer equilibrium was regained rapidly. When $k_{\text{for}}(\text{H})$ values for relaxation were plotted against DABCO concentration (Fig. 3c), a simple linear (*i.e.* first order) correlation was observed, giving the second-order rate constant, $k_2 = 9.13 \times 10^2 \text{ M}^{-1} \text{ s}^{-1}$. In terms of basicity, DABCO ($\text{p}K_{\text{aH}}(\text{MeCN}) = 18.29$)⁵² is insufficiently basic to quantitatively deprotonate **4a-keto** (for **4a-keto** estimated $\text{p}K_{\text{a}}(\text{MeCN}) = \text{p}K_{\text{a}}(\text{DMSO}) + 12.9$ (ref. 53) = 13.4 (ref. 54) + 12.9 = 26.3). Thus our data suggest that DABCO may operate as a general base catalyst.

Upon delivery of electrophilic fluorine, N-F reagents give amines as by-products, which could promote keto-enol tautomerism, and hence the rate of fluorination, if they remain unprotonated. Fluorination reactions using Selectfluor™ result in the formation of $\text{ClCH}_2\text{-DABCO}^+\text{BF}_4^-$ and when 0.5 to 2 equivalents of $\text{ClCH}_2\text{-DABCO}^+\text{BF}_4^-$ were added to **4a-keto**, very small (1.4 to 2-fold) increases in k_{obs} and $k_{\text{for}}(\text{H})$ were observed (Fig. 3d). However, the addition of greater quantities of $\text{ClCH}_2\text{-DABCO}^+\text{BF}_4^-$ (25–100 equivalents) resulted in reduced $k_{\text{for}}(\text{H})$ values (see ESI Section 3.4.5†). For example, with 100 equivalents of $\text{ClCH}_2\text{-DABCO}^+$, $k_{\text{for}}(\text{H})$ was reduced three-fold. While the $\text{ClCH}_2\text{-DABCO}^+$ cation is unlikely to remain unprotonated and thus will be unable to function as a base, this series of experiments suggested the possibility of salt effects upon the



Table 1 Summary of ketone relaxation of non-fluorinated 1,3-dicarbonyl systems. The k_{obs} values for relaxation of photo-ketonized forms of **4a–d** (0.025 mM) were determined in MeCN at 20 °C in the presence of additives. Percentages represent volumes of additive in MeCN. Equilibrium constants K_e were determined by NMR spectroscopy or by linear interpolation, extrapolation or averaging of the measured data. Forward and reverse rate constants, $k_{\text{for}}(\text{H})$ and $k_{\text{rev}}(\text{H})$, for enolization and ketonization processes, of the non-fluorinated 1,3-dicarbonyl systems, respectively were calculated using eqn (1) and (2)

Aryl substituent	Additive	Quantity of additive	$k_{\text{obs}}/\text{s}^{-1}$	Approx. $t_{1/2}$	$K_e(\text{H})$	$k_{\text{for}}(\text{H})/\text{s}^{-1}$	$k_{\text{rev}}(\text{H})/\text{s}^{-1}$	$k_{\text{for}}(\text{H})\{ \text{with additive}\}/k_{\text{for}}(\text{H})\{\text{MeCN}\}$
4a (R = H)	None	—	7.26 × 10 ⁻⁵	2.7 h	10.5 ^a	6.63 × 10 ⁻⁵	6.31 × 10 ⁻⁶	1.0
	Water	15%	8.44 × 10 ⁻⁵	2.3 h	7.8 ^c	7.48 × 10 ⁻⁵	9.59 × 10 ⁻⁶	1.1
		20%	1.79 × 10 ⁻⁴	1.1 h	6.9 ^b	1.56 × 10 ⁻⁴	2.27 × 10 ⁻⁵	2.4
		25%	1.84 × 10 ⁻⁴	1 h	6.6 ^c	1.60 × 10 ⁻⁴	2.42 × 10 ⁻⁵	2.4
		35%	3.39 × 10 ⁻⁴	34 min	6.3 ^c	2.93 × 10 ⁻⁴	4.64 × 10 ⁻⁵	4.4
		50%	7.29 × 10 ⁻⁴	15 min	5.7 ^b	6.20 × 10 ⁻⁴	1.09 × 10 ⁻⁴	9.4
	Formic acid	0.5%	1.92 × 10 ⁻³	6 min	10.3 ^c	1.75 × 10 ⁻³	1.70 × 10 ⁻⁴	26
		1%	4.16 × 10 ⁻³	3 min	10.0 ^b	3.78 × 10 ⁻³	3.78 × 10 ⁻⁴	57
		2%	4.89 × 10 ⁻³	2 min	10.5 ^b	4.46 × 10 ⁻³	4.25 × 10 ⁻⁴	67
		3%	6.29 × 10 ⁻³	2 min	9.5 ^b	5.69 × 10 ⁻³	5.99 × 10 ⁻⁴	86
	DABCO	2.5 μM	2.92 × 10 ⁻³	4 min	6.7 ^c	2.54 × 10 ⁻³	3.80 × 10 ⁻⁴	39
		12.5 μM	1.34 × 10 ⁻²	1 min	6.7 ^c	1.17 × 10 ⁻²	1.74 × 10 ⁻³	176
		25 μM (1 eq.)	2.49 × 10 ⁻²	30 s	6.7 ^b	2.17 × 10 ⁻²	3.24 × 10 ⁻³	327
		37.5 μM	4.08 × 10 ⁻²	17 s	6.7 ^c	3.55 × 10 ⁻²	5.30 × 10 ⁻³	536
		50 μM	5.22 × 10 ⁻²	13 s	6.7 ^b	4.54 × 10 ⁻²	6.78 × 10 ⁻³	685
	$\text{ClCH}_2\text{-DABCO}^+\text{BF}_4^-$	12.5 μM	1.04 × 10 ⁻⁴	2 h	9.1 ^c	9.37 × 10 ⁻⁵	1.03 × 10 ⁻⁵	1.4
		25 μM (1 eq.)	1.20 × 10 ⁻⁴	1.6 h	9.1 ^b	1.08 × 10 ⁻⁴	1.19 × 10 ⁻⁵	1.6
		50 μM	1.32 × 10 ⁻⁴	1.5 h	9.1 ^c	1.19 × 10 ⁻⁴	1.31 × 10 ⁻⁵	1.8
		62.5 μM	1.00 × 10 ⁻⁴	2 h	9.1 ^c	9.01 × 10 ⁻⁵	9.90 × 10 ⁻⁶	1.4
		1.25 mM	5.12 × 10 ⁻⁵	4 h	9.1 ^c	4.61 × 10 ⁻⁵	5.07 × 10 ⁻⁶	0.7
		2.5 mM	2.04 × 10 ⁻⁵	9 h	9.1 ^c	1.84 × 10 ⁻⁵	2.02 × 10 ⁻⁶	0.3
		20% water and $\text{ClCH}_2\text{-DABCO}^+\text{BF}_4^-$	2.05 × 10 ⁻⁴	1 h	6.9 ^c	1.79 × 10 ⁻⁴	2.59 × 10 ⁻⁵	2.7
		$^n\text{Bu}_4\text{N}^+\text{BF}_4^-$	1.44 × 10 ⁻⁴	1.3 h	9.1 ^b	1.30 × 10 ⁻⁴	1.43 × 10 ⁻⁵	2.0
4b (R = OMe)	None	—	1.29 × 10 ⁻⁵	15 h	4.0 ^a	1.03 × 10 ⁻⁵	2.58 × 10 ⁻⁶	1.0
	Water	50%	1.47 × 10 ⁻⁴	1.3 h	3.7 ^b	1.16 × 10 ⁻⁴	3.13 × 10 ⁻⁵	1.1
	Formic acid	2%	8.27 × 10 ⁻³	1.4 min	5.3 ^b	6.96 × 10 ⁻³	1.31 × 10 ⁻³	674
	DABCO	2.5 μM	8.24 × 10 ⁻⁴	14 min	5.1 ^b	6.89 × 10 ⁻⁴	1.35 × 10 ⁻⁴	67
		50 μM	7.11 × 10 ⁻⁶	27 h	5.0 ^b	5.93 × 10 ⁻⁶	1.19 × 10 ⁻⁶	0.6
4c (R = Me)	None	—	5.67 × 10 ⁻⁵	3.5 h	8.0 ^a	5.04 × 10 ⁻⁵	6.30 × 10 ⁻⁶	1.0
	Water	50%	3.15 × 10 ⁻⁴	37 min	8.0 ^d	2.80 × 10 ⁻⁴	3.50 × 10 ⁻⁵	5.6
	DABCO	2.5 μM	8.03 × 10 ⁻⁴	14 min	8.0 ^d	7.14 × 10 ⁻⁴	8.92 × 10 ⁻⁵	14
4d (R = Cl)	None	—	1.07 × 10 ⁻⁴	2 h	12.5 ^a	9.91 × 10 ⁻⁵	7.93 × 10 ⁻⁶	1.0
	Water	50%	2.13 × 10 ⁻³	5 min	12.5 ^d	1.97 × 10 ⁻³	1.58 × 10 ⁻⁴	20
	DABCO	2.5 μM	7.69 × 10 ⁻³	1.5 min	12.5 ^d	7.12 × 10 ⁻³	5.70 × 10 ⁻⁴	72
		25 μM	7.35 × 10 ⁻⁵	2.6 h	12.5 ^d	6.81 × 10 ⁻⁵	5.44 × 10 ⁻⁶	0.7

^a Measured by ¹H NMR spectroscopy in MeCN-*d*₃. ^b Measured by ¹H NMR spectroscopy in MeCN-*d*₃ in the presence of additive (for details see ESI Section 3.2†). ^c Value based on average of measured values or interpolation of measured values. ^d $K_e(\text{H})$ value was assumed to be the same as $K_e(\text{H})$ in MeCN-*d*₃ alone.

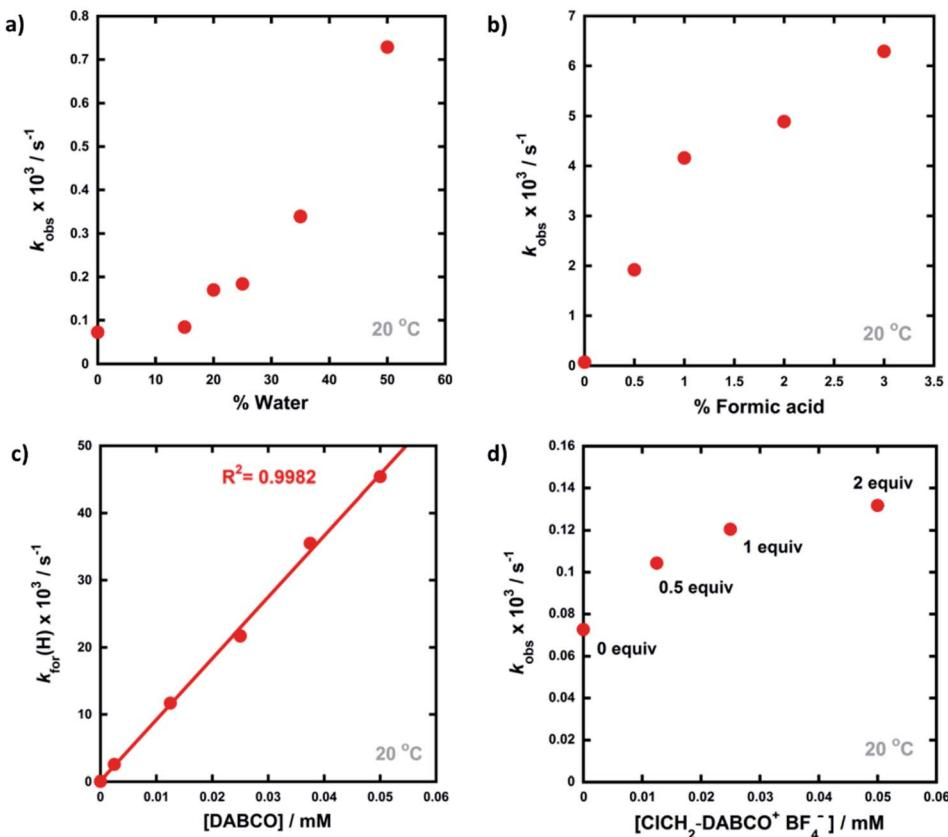


Fig. 3 Trends observed in the rates of relaxation (k_{obs}) of **4a** (0.025 mM) upon addition of different quantities of additives, in MeCN at 20 °C: (a) water, (b) formic acid, (c) DABCO, (d) 0.5–2 equivalents of $\text{ClCH}_2\text{-DABCO}^+\text{BF}_4^-$.

relaxation processes. Consequently, relaxation experiments were performed in the presence of 2–100 equivalents of LiBF_4 and similar reductions in $k_{\text{for}}(\text{H})$ were observed (for related spectra see ESI Section 3.4.7†). Li salts are known to form chelates with 1,3-diketones,⁵⁴ thus we explored the effects of adding ${}^7\text{Bu}_4\text{NBF}_4$, a non-chelating salt. In order to mimic the salt concentrations in synthetic-scale processes, we studied the effect of adding 240 mM ${}^7\text{Bu}_4\text{NBF}_4$ to solutions of **4a-keto**. Under these conditions, $k_{\text{for}}(\text{H})$ increased 2-fold in comparison to experiments in the absence of salts. In summary, the effects of ‘spent’ Selectfluor™ (*i.e.* $\text{ClCH}_2\text{-DABCO}^+\text{BF}_4^-$) and other ionic species upon enolization kinetics of **4a–d** are measurable, but marginal and potentially complex in nature.

We also explored the effects of the amine derivative of NFSI, dibenzenesulfonimide ($(\text{PhSO}_2)_2\text{NH}$, $\text{pK}_a(\text{MeCN}) \sim 11.3$)⁵⁵ upon the rate of relaxation of **4a-keto**. Interestingly, the presence of 5 equivalents of $(\text{PhSO}_2)_2\text{NH}$ resulted in a 40-fold decrease in the relaxation rate constant rate, however, 10 equivalents of $(\text{PhSO}_2)_2\text{NH}$ gave only a 16-fold decrease (see ESI Section 3.4.8–3.4.9†). The addition of the conjugate base form, $(\text{PhSO}_2)_2\text{N}^-\text{Na}^+$, also showed a similar effect, with one equivalent causing a significant reduction in relaxation rate and larger concentrations showing less-pronounced reductions. In this case, the reduction in $k_{\text{for}}(\text{H})$ is likely due to chelation of the Na^+ ion to diketone **4a**, an interaction previously described by Bordwell.⁵⁴

The relaxation kinetics of keto forms of **4b–d** were explored using the same photoketonization procedure, in the presence and absence of additives, and corresponding k_{obs} , K_e , $k_{\text{for}}(\text{H})$ and $k_{\text{rev}}(\text{H})$ values are reported in Table 1. There were little variations in measured K_e values for **4b** across the range of conditions that we employed. For **4c** and **4d**, we assumed that the $K_e(\text{H})$ values in the presence of additives would be the same as $K_e(\text{H})$ in $\text{MeCN-}d_3$ alone under conditions where measured values were not obtained. The effects of the *para*-substituents within **4a–d** on $k_{\text{for}}(\text{H})$ in MeCN were studied by Hammett correlation analysis. The use of σ_p^+ values in the construction of the Hammett plot gave better correlations than with σ_p values (see ESI Section 3.5†). A ρ^+ value of +1.06 was obtained, where this positive value indicates small increases in electron density on the aryl rings of the substrates during the limiting C–H removal step of enolization. Compound **4d** ($\text{R} = \text{Cl}$) relaxed most rapidly, whereas compound **4b** ($\text{R} = \text{OMe}$) was the slowest, which suggests that rate limiting proton transfer from carbon proceeds towards an anionic intermediate rather than through pre-protonation of the ketone.

2.2 Kinetics of keto-enol tautomerism in compounds **5a–d**

Compounds **5a–d** were synthesised using our previously reported methods,³⁷ in good yields. Following purification by recrystallization, we obtained the fluorinated 1,3-diaryl-1,3-dicarbonyls as mixtures of both keto and enol tautomers,

where the keto form comprised $\sim 95\%$ of **5a** and **5b**, and $\sim 90\%$ of **5c** and **5d** (as determined by ^{19}F NMR spectroscopy in MeCN- d_3 , see ESI Section 3.2†). We determined K_e values for **5a** across a range of additives and, in a similar vein to the non-fluorinated systems, we found K_e to be broadly constant. The fluoroenol- and fluoroketo-tautomers of **5a-d** have distinct absorbance bands at ~ 350 nm and ~ 250 nm, respectively. Therefore, in much the same way as for compounds **4a-d**, we were able to monitor the tautomerism processes of the fluorinated derivatives *via* changes in absorbance of the fluoroenol tautomers. Photoketonization experiments were conducted on 0.50 mM solutions of **5a-d** in MeCN in the absence of additives (Fig. 4a). Following irradiation, spectrophotometric kinetic assays for relaxation were conducted, and they showed very slow restoration of the thermodynamic ratio between the two tautomeric forms. Plots of diketone concentration *versus* time for **5a-d** were constructed. In the case of **5a** and **5d** (Fig. 4b and c), sigmoidal behaviours were clearly discernible, which suggested autocatalysis of the processes, and fitting of the data to a model for reversible autocatalysis gave strong support for this hypothesis (for kinetic fittings performed using Wolfram Mathematica see ESI Sections 3.9.1 and 3.12.1†). In the case of **5b** and **5c**, reaction progress was extremely slow, and k_{obs} values were estimated using an initial rates approach (see ESI Sections 3.10.1 and 3.11.1†).

We then explored the effects of additives on the rates of relaxation of diketone tautomers of **5a-d**, and the corresponding $k_{\text{for}}(\text{F})$ and $k_{\text{rev}}(\text{F})$ values were obtained *via* K_e values (Table 2). In general, the effects of additives upon $k_{\text{for}}(\text{F})$ were much greater than for the non-fluorinated series **4a-d**. With 20%

water in MeCN, **5a-keto** $k_{\text{for}}(\text{F})$ was 160-fold larger than in the absence of water, whereas for system **4a-keto**, only a 2.4-fold enhancement in $k_{\text{for}}(\text{H})$ was observed. When the quantity of water in MeCN was increased to 50%, $k_{\text{for}}(\text{F})$ for **5a-keto** was further increased to 930-fold greater than in the absence of water. For compounds **5b** and **5d**, $k_{\text{for}}(\text{F})$ increased 3000-fold in 50% water, while **5c** showed a 10 000-fold increase. Addition of formic acid (3% in MeCN) led to an increase in $k_{\text{for}}(\text{F})$ of 220-fold, whereas DABCO proved to be an effective agent for defluorination of the substrate **5a** (see ESI Section 3.2.1† for related spectra, and previous reports^{56,57} of bromomalonitriles acting as brominating agents). ‘Spent’ SelectfluorTM (ClCH₂-DABCO⁺BF₄⁻, 0.025 mM) offered a 4-fold increase in $k_{\text{for}}(\text{F})$, whereas the increase in $k_{\text{for}}(\text{H})$ for **4a** with this additive was ~ 2 -fold, and only marginally discernible above salt-related medium effects (see ESI Section 3.9† for spectra).

Overall, these data suggest that the tautomerization reactions of the fluoro-systems **5a-d** are accelerated much more significantly in the presence of polar additives than those of the non-fluorinated systems.

2.3 Kinetics of enol and fluoroenol fluorination

We previously reported the kinetics of fluorination of enols **4a-d** in MeCN.³⁷ We confirmed that fluorination of **5a** occurs only *via* the fluoroenol form with the aid of NMR experiments, and that the fluoroketo tautomer acts as a spectator during the addition of the second fluorine atom to **5a-enol**, owing to its slow enolization in MeCN. Here we explore the effects of additives upon the rates of fluorination of enols **4a-d** and make comparisons with their effects upon the rates of fluorination of

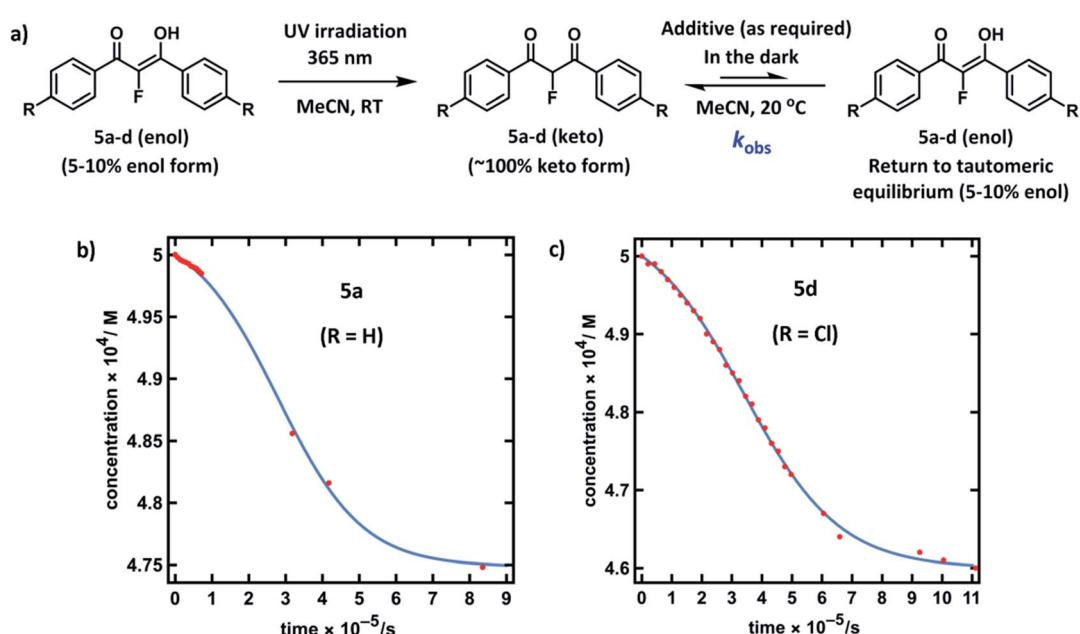


Fig. 4 (a) Reaction scheme for photoketonization (step 1) by irradiation with a 0.5 W UV LED lamp at 365 nm for 4–5 hours, followed by relaxation (step 2) of **5a-d** in MeCN. (b) Plot of $[\text{5a-keto}]$ *versus* time obtained from a time-arrayed single-wavelength kinetic analysis for relaxation of **5a-keto** showing the return to the tautomeric equilibrium (0.50 mM, 20 °C, spectra acquired over 11 days). (c) Plot of $[\text{5d-keto}]$ *versus* time obtained from a time-arrayed single-wavelength kinetic analysis for relaxation of **5d-keto** showing the return to the tautomeric equilibrium (0.50 mM, 20 °C, spectra acquired over 13 days).



Table 2 Summary of diketone relaxation of 2-fluorinated-1,3-dicarbonyl systems. The k_{obs} values for relaxation of photoketonized forms of **5a–d** (0.50 mM) were determined in MeCN at 20 °C in the presence of additives. Percentages represent volumes of additive in MeCN. Equilibrium constants K_e were determined by NMR spectroscopy or by linear interpolation, extrapolation or averaging of the measured data. Forward and reverse rate constants, $k_{\text{for}}(\text{F})$ and $k_{\text{rev}}(\text{F})$, for enolization and ketonization processes, of the 2-fluorinated-1,3-dicarbonyl systems, respectively were calculated using eqn (1) and (2)

Aryl substituent	Additive	Quantity of additive	$k_{\text{obs}}/\text{s}^{-1}$	Approx. $t_{1/2}$	$K_e(\text{F})$	$k_{\text{for}}(\text{F})/\text{s}^{-1}$	$k_{\text{rev}}(\text{F})/\text{s}^{-1}$	$k_{\text{for}}(\text{F})\{\text{with additive}\}/$
								$k_{\text{for}}(\text{F})\{\text{MeCN}\}$
5a (R = H)	None	—	— ^a	—	0.053 ^b	3.66 × 10 ⁻⁸ [1.58 × 10 ⁻²] ^c	6.91 × 10 ⁻⁷ (0.298) ^c	1.0
	Water	10%	4.98 × 10 ⁻⁵	4 h	0.053 ^d	2.49 × 10 ⁻⁶	4.73 × 10 ⁻⁵	68
		20%	1.19 × 10 ⁻⁴	1.6 h	0.053 ^{d,e}	5.95 × 10 ⁻⁶	1.13 × 10 ⁻⁴	163
		30%	2.23 × 10 ⁻⁴	0.9 h	0.053 ^d	1.12 × 10 ⁻⁵	2.12 × 10 ⁻⁴	305
		40%	3.77 × 10 ⁻⁴	0.5 h	0.053 ^d	1.89 × 10 ⁻⁵	3.58 × 10 ⁻⁴	515
		50%	6.78 × 10 ⁻⁴	0.3 h	0.053 ^b	3.39 × 10 ⁻⁵	6.44 × 10 ⁻⁴	926
		3%	1.64 × 10 ⁻⁴	1.2 h	0.053 ^b	8.20 × 10 ⁻⁶	1.56 × 10 ⁻⁴	224
	DABCO	2.5 μM	1.42 × 10 ⁻³	8 min	— ^f	— ^f	— ^f	— ^f
	ClCH ₂ -DABCO ⁺ BF ₄ [−]	12.5 μM	1.01 × 10 ^{−6}	8 d	0.053 ^d	5.05 × 10 ^{−8}	9.60 × 10 ^{−7}	1.4
	25 μM (1 eq.)	2.93 × 10 ^{−6}	2.7 d	0.053 ^d	1.47 × 10 ^{−7}	2.78 × 10 ^{−6}	4.0	4.0
5b (R = OMe)	20% water and ClCH ₂ -DABCO ⁺ BF ₄ [−]	1.91 × 10 ^{−4}	1 h	0.053 ^d	9.55 × 10 ^{−6}	1.81 × 10 ^{−4}	261	261
	<i>n</i> Bu ₄ N ⁺ BF ₄ [−]	8.38 × 10 ^{−5}	2.3 h	0.043 ^g	3.42 × 10 ^{−6}	8.04 × 10 ^{−5}	94	94
	—	—	1.46 × 10 ^{−7} ^h	60 d	0.020 ^b	2.92 × 10 ^{−9} (n.d.) ^c	1.43 × 10 ^{−7} (n.d.) ^c	1.0
	Water	20%	3.22 × 10 ^{−5}	6 h	0.033 ^d	1.04 × 10 ^{−6}	3.12 × 10 ^{−5}	355
		30%	5.39 × 10 ^{−5}	3.6 h	0.040 ^d	2.06 × 10 ^{−6}	5.18 × 10 ^{−5}	706
		40%	9.23 × 10 ^{−5}	2.1 h	0.046 ^d	4.07 × 10 ^{−6}	8.82 × 10 ^{−5}	1396
		50%	1.71 × 10 ^{−4}	1.1 h	0.053 ^b	8.55 × 10 ^{−6}	1.62 × 10 ^{−4}	2928
		2%	1.73 × 10 ^{−5}	11 h	0.031 ^b	5.19 × 10 ^{−7}	1.68 × 10 ^{−5}	178
	DABCO	2.5 μM	1.32 × 10 ^{−5}	15 h	0.020 ^b	2.64 × 10 ^{−7}	1.29 × 10 ^{−5}	90
	—	—	8.64 × 10 ^{−8} ^h	90 d	0.149 ^b	1.12 × 10 ^{−8}	7.52 × 10 ^{−8}	1.0
5c (R = Me)	None	—	9.15 × 10 ^{−4}	0.2 h	0.149 ⁱ	1.19 × 10 ^{−4}	7.96 × 10 ^{−4}	10 594
	Water	50%	— ^a	1.97 × 10 ^{−3}	6 min	0.087 ^b	5.37 × 10 ^{−8} [1.11 × 10 ^{−2}] ^c	6.18 × 10 ^{−7} (0.128) ^c
5d (R = Cl)	None	—	— ^a	—	0.087 ⁱ	1.58 × 10 ^{−4}	1.81 × 10 ^{−3}	2936
	Water	50%	—	—	0.087 ⁱ	1.58 × 10 ^{−4}	1.81 × 10 ^{−3}	2936

^a System displayed non-first order autocatalytic behaviour. ^b Measured by ¹⁹F NMR spectroscopy in MeCN-*d*₃ or MeCN-*d*₃/D₂O. ^c Second order rate constant for autocatalytic process in units of M^{−1} s^{−1}.

^d Value based on average of measured values or interpolation of measured values. ^e A ¹⁹F NMR spectroscopy measurement in 20% H₂O/MeCN-*d*₃ gave $K_e(\text{F}) = 0.042$. ^f Det fluorination was observed. ^g Measured in the presence of 300 mM *n*Bu₄N⁺BF₄[−]. ^h Extremely slow process, where rate constant was determined by initial rates method. ⁱ $K_e(\text{F})$ for 50% H₂O was assumed to be the same as $K_e(\text{F})$ in MeCN-*d*₃.

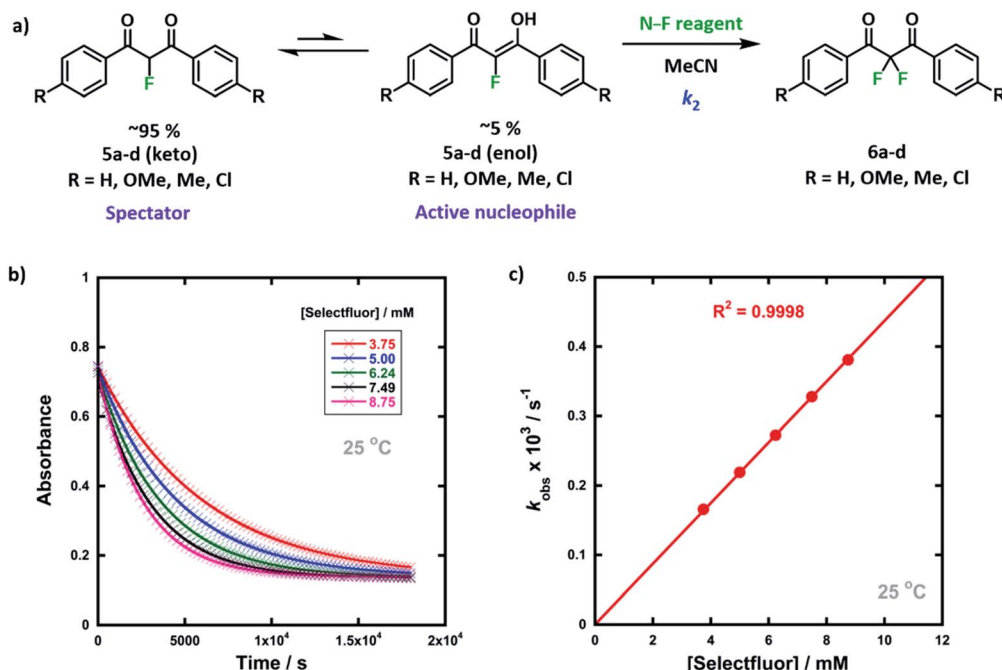


Fig. 5 (a) Reaction scheme for fluorination reactions of 1,3-dicarbonyls **5a–d** with Selectfluor™ or NFSI in MeCN at controlled temperatures. (b) Exponential decays of absorbance of **5a-enol** at 350 nm with different concentrations of Selectfluor™, in MeCN at 25 °C. (c) Correlation of k_{obs} values for fluorination of **5a-enol** with [Selectfluor™], in MeCN at 25 °C.

fluoroenols **5a–d**. Together, these data allow us to explore the role of 2-fluorination upon enol nucleophilicity and potentially tune conditions, through the addition of *e.g.* water, towards favouring the formation of 2,2-difluoro-1,3-dicarbonyls **6a–d** (Fig. 5a). Furthermore, on account of the greatly increased rates of enolization in the presence of additives, we also take account of *in situ* enolization of **5a**.

By monitoring the decays in absorbance of the fluoroenol tautomers of **5a–d** at $\lambda \sim 350$ nm, the kinetics of fluorination reactions were conveniently monitored by UV-vis spectrophotometry. To achieve pseudo-first order conditions, all kinetics experiments were carried out using excess electrophile. Clean exponential decays of absorbance of the nucleophile were observed in all runs in MeCN alone (representative examples are shown in Fig. 5). The first-order rate constants k_{obs} were obtained from the fitting of plots of absorbance *versus* time (Fig. 5b). When k_{obs} values were plotted against electrophilic fluorine concentration, linear (*i.e.* first order) correlations were observed (Fig. 5c), which projected cleanly through the origin in each case. The direct dependence upon electrophilic fluorine concentration demonstrates rate-limiting fluorination of the fluoroenol that is present in the mixture, and thus the slopes of these graphs gave the second-order rate constant k_2 [$\text{M}^{-1} \text{ s}^{-1}$] according to the rate eqn (3). The rate constants for the reactions of **5a–d** with each fluorinating reagent are summarized in Table 3.

$$\text{Rate} = \frac{d[\text{Fluoroenol}]}{dt} = -k_2[\text{Fluoroenol}][\text{N–F reagent}] \quad (3)$$

A Hammett plot was constructed for the reactions of fluoroenols **5a–d** with Selectfluor™ 1 (see ESI Section 3.13.5†). The

use of σ_p^+ values led to a better correlation than with σ_p constants, and $\rho^+ = -1.5$ was obtained, with R^2 of > 0.99 . This value is similar to the ρ^+ values we obtained for fluorination of enols **4a–d** by several N–F reagents, including Selectfluor™ 1 and NFSI 2.³⁷ Activation parameters (ΔG^\ddagger , ΔH^\ddagger and ΔS^\ddagger) were calculated from kinetic data obtained at different temperatures for the reactions of Selectfluor™ with **5a-enol** and **5b-enol** (see ESI Section 3.13.5†). As with our previous publication, the moderately negative values of ΔS^\ddagger , alongside the values for ρ^+ , support an $\text{S}_{\text{N}}2$ -type mechanism for the fluorination reactions.

The rates of fluorination of **5a–d** by Selectfluor™ 1 and NFSI 2 were compared with the rate constants that we previously obtained for the fluorinations of **4a–d**,³⁷ using k_{rel} values, defined in eqn (4).

Table 3 Second-order rate constants (k_2) for the reactions of Selectfluor™ 1 and NFSI 2 with nucleophiles **5a–d**, in MeCN at 25 °C, and relative rates compared to the reactions of Selectfluor™ and NFSI with **4a–d**

Nucleophile	Electrophile	k_2 (25 °C)/ $\text{M}^{-1} \text{ s}^{-1}$	k_{rel}
5a-enol (R = H)	Selectfluor™ 1	4.37×10^{-2}	1.0 (1.1) ^a
	NFSI 2	4.59×10^{-4}	46
5b-enol (R = OMe)	Selectfluor™ 1	6.77×10^{-1}	1.1 (1.1) ^a
	NFSI 2	6.11×10^{-4}	4.4
5c-enol (R = Me)	Selectfluor™ 1	1.32×10^{-1}	1.1
	NFSI 2	2.47×10^{-4}	43
5d-enol (R = Cl)	Selectfluor™ 1	3.07×10^{-2}	1.7
	NFSI 2	2.47×10^{-4}	43

^a Using k_2 values for reactions measured at 20 °C.



$$k_{\text{rel}} = \frac{k_2 \text{ (addition of second fluorine atom)}}{k_2 \text{ (addition of first fluorine atom)}} \quad (4)$$

The k_2 values obtained for fluorination of fluoroenols **5a-d** by Selectfluor™ are slightly higher than those for fluorination of enols **4a-d**, with k_{rel} values of 1.0–1.7 being observed. With NFSI, the rate enhancement is more pronounced, and the addition of the second fluorine atom to form the CF_2 group is 46-fold faster for **5a-enol**, 4-fold greater for **5b-enol** and 43-fold faster for **5d-enol**.

One might expect that the presence of a highly electronegative fluorine atom would lead to a lowering of the nucleophilicity of the fluoroenol and much lower rates of fluorination. On the other hand, the strong pi-donor ability of the fluorine atom could lead to ground-state destabilization of fluorine atoms at sp^2 centres and thus enhanced nucleophilicity of the fluoroenol. Our results suggest that a balance between these opposing effects is observed for fluorinations in MeCN with the more reactive Selectfluor™ system, however, with the less reactive NFSI reagent the fluoroenols **5a-d** are more reactive. The origins of this disparity could lie in the less early transition state structure that is to be expected from the less reactive NFSI system, coupled with the different charge state of the electrophile–nucleophile pair, and thus differing requirements for solvation.

Our findings of enhanced nucleophilicity for fluoroenols **5a-d** over enols **4a-d** align with studies conducted by Dolbier *et al.*^{58–60} on the kinetic impact of vinylic fluorine substituents upon cyclization reactions. They reported that the presence of a fluorine atom at an sp^2 centre was disfavoured relative to the sp^3 hybridised analogue, therefore, cyclization reactions occurred readily to form butadiene compounds. Chambers *et al.*^{13,14} reported that during electrophilic fluorination by elemental fluorine, the second fluorination step is much slower than the first. However, our results show that addition of the second fluorine atom proceeds at a rate that is similar to or even greater than the first fluorination step. The previously reported slow rate of difluorination is due to rate-limiting enolization of the mono-fluoro-diketone compound rather than the fluorination process itself. As we have shown in Section 2.2, the rate of enolization can be enhanced by the addition of catalytic amounts of water, salt, acid or base, which in turn contributes to an increase in the overall rate of the difluorination mechanism. Furthermore, in related carbanion systems, the reactivity was found to be enhanced by the presence of an α -fluorine atom compared to the non-fluorinated carbanion.^{61,62} Indeed, the effect of the α -fluorine was even greater in these studies, probably because of the increased repulsion between the oxyanionic charge and fluorine lone pairs in comparison to our systems.

We also studied the fluorinations of **4a-enol** and **5a-enol** by Selectfluor™ with 20% water in MeCN using an initial rates approach to overcome the complications associated with the presence of substantial keto-enol tautomerization and the formation of the hydrate of **6a** under these conditions (for spectra see ESI Sections 3.15 and 3.18†). The presence of water (20% in MeCN) during the fluorination of **5a-enol** gave a ~50-

fold larger second-order rate constant, k_2 , compared to without water, however, the k_2 value for fluorination of **4a-enol** was little changed (Table 4). We also explored the effects of adding formic acid (3–20%) on the rates of fluorination of **5a-enol** and found that there was little effect on the k_2 values (see ESI Section 3.16†). The presence of $^n\text{Bu}_4\text{NBF}_4$ (240 mM) during the fluorination of **5a-enol** by Selectfluor™ afforded a ~2600-fold increase in rate, where this large increase is likely due to the combined effects of the salt itself and inadvertent addition of water owing to the hygroscopic nature of tetraalkylammonium systems.⁶³ Taken together, the effects of additives upon k_2 further support the idea of differential solvation and medium effects along the reaction co-ordinates of the fluorination and tautomerization processes of the enol and fluoroenol systems, however, their underlying origins are not clear at this stage.

2.4 Application of kinetic data to synthesis

Our kinetic studies show that additives, such as water, facilitate enolization of 1,3-dicarbonyl species **4** and **5**, with especially dramatic effects upon 2-fluoro-1,3-dicarbonyls **5**. The presence of additives also has clear effects on the fluorination processes of **4a** and **5a** with Selectfluor™. In order to demonstrate the quantitative applicability of our data to synthetic scenarios, both in the presence and absence of water, we performed NMR experiments (Fig. 6a–d) to monitor the kinetics of fluorination of **4a** with Selectfluor™ and compared measured data with a numerically-solved differential model (Fig. 7a–c) of the overall processes based upon the microscopic rate constants we have determined.

In MeCN-*d*₃ alone, we reacted **4a** (30 mM) with Selectfluor™ **1** (2.1 equivalents) and the evolution of species was monitored by ¹⁹F NMR spectroscopy over 6 days. Without water, **5a-keto** ($\delta = -190$ ppm) was formed rapidly from the large reservoir of **4a-enol** (~90% of total **4a**), with a second kinetic phase of **5a-keto** formation associated with enolization of residual **4a-keto** (Fig. 6a and green dots in Fig. 6c). On the basis of our UV-vis kinetic data, the formation of **5a-enol** was expected to be extremely slow, with the formation of **6a** ($\delta = -103$ ppm) being similarly slow as a result. This was borne out by the very slow appearance of 2,2-difluoro-1,3-dicarbonyl **6a**, with its formation only being evident at a level of ~4% after 5 days.

The reaction conducted with 20% H₂O in MeCN-*d*₃ allowed for the use of higher concentrations of Selectfluor™ owing to its enhanced solubility in this medium, thus concentrations of **4a** = 60 mM and Selectfluor™ = 125 mM were used. The reaction

Table 4 Second-order rate constants (k_2) for the reactions of Selectfluor™ with nucleophiles **4a-enol** and **5a-enol** in 20% water in MeCN at 20 °C

Nucleophile	k_2 (20 °C)/M ⁻¹ s ⁻¹
4a-enol (R = H)	2.49×10^{-2a}
5a-enol (R = H)	1.43^b

^a In MeCN only, $k_2 = 2.68 \times 10^{-2}$ M⁻¹ s⁻¹ at 20 °C for fluorination of **4a-enol**.³⁷ ^b At 20 °C in MeCN only, $k_2 = 2.95 \times 10^{-2}$ M⁻¹ s⁻¹ for fluorination of **5a-enol**.



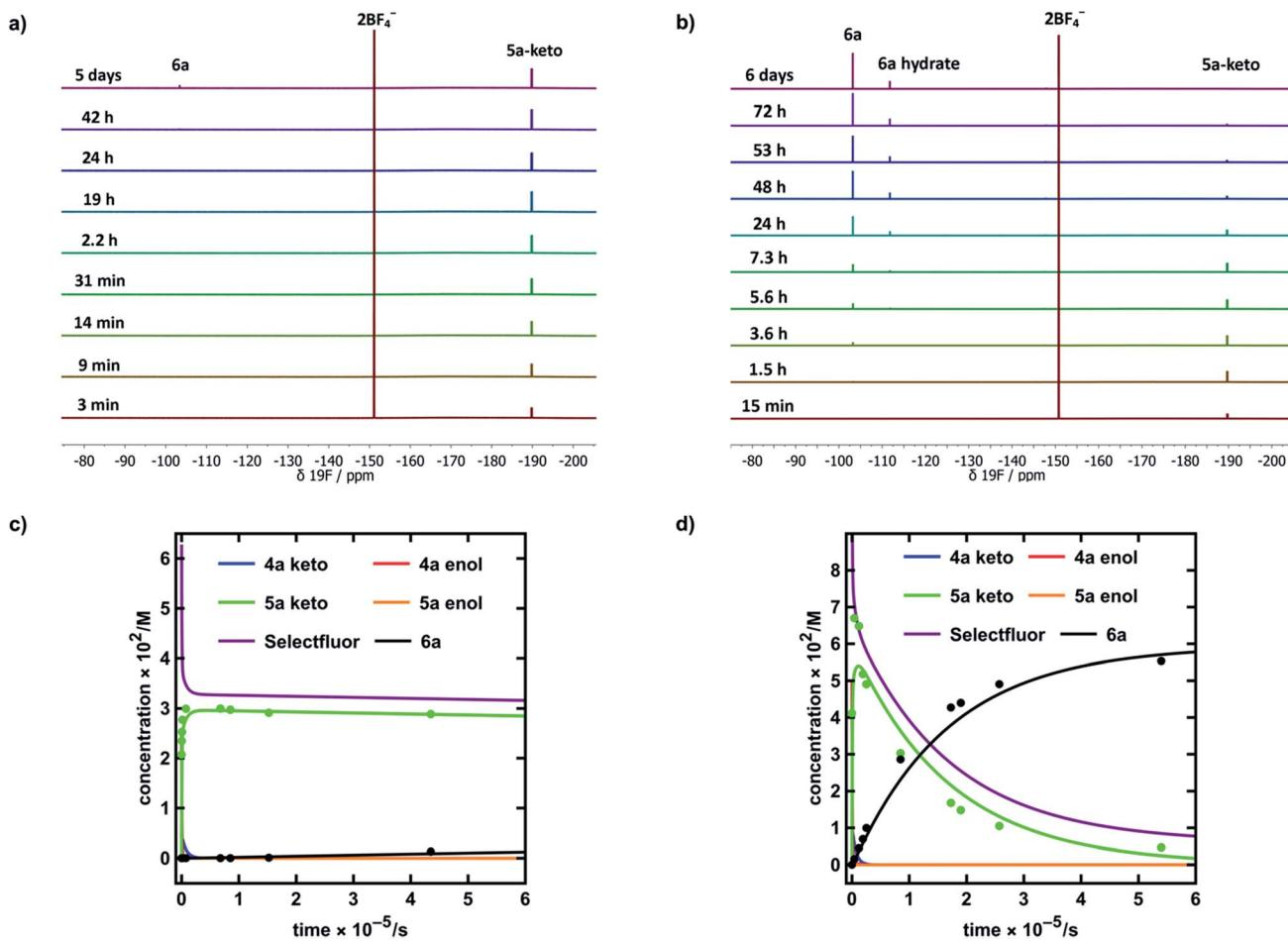


Fig. 6 (a) ^{19}F NMR time profile for the reaction between 1,3-dicarbonyl **4a** (30 mM) and Selectfluor™ (62.5 mM) in $\text{MeCN-}d_3$. (b) ^{19}F NMR time profile for the reaction between 1,3-dicarbonyl **4a** (59.5 mM) and Selectfluor™ (125 mM) in 20% water in $\text{MeCN-}d_3$. (c) Integrated ^{19}F NMR-time data for the reaction between **4a** (30 mM) and Selectfluor™ (62.5 mM) in $\text{MeCN-}d_3$. (d) Integrated ^{19}F NMR-time data for the reaction between **4a** (59.5 mM) and Selectfluor™ (125 mM) in 20% water in $\text{MeCN-}d_3$. Some over-estimation of the concentration of **5a**-keto was evident in the NMR experiment and the origin of this is discussed further in the ESI Section 4.†

profile showed rapid build-up of **5a**-keto ($\delta = -190$ ppm) as a result of the large starting concentration of **4a**-enol. Owing to the presence of water, enolization of **5a**-keto was expected to occur more readily, and this was evidenced by the more rapid reduction in the signal for **5a**-keto (Fig. 6b and green dots in Fig. 6d) and the formation of 7.5% **6a** ($\delta = -103$ ppm) after ~ 3.5 h (Fig. 6d black dots), with complete conversion to **6a** being achieved over 6 days (fluorination was expected to be rapid, and this was supported by very low levels of **5a**-enol being detected in the steady state). An additional peak was present at $\delta = -111.9$ ppm (Fig. 6b) which is likely to correspond to a hydrate of **6a**. The formation of a hydrate is expected, as difluoroketones are known to form stable tetrahedral adducts.³² We also observed this peak in our ^{19}F NMR-monitored synthetic reaction to obtain an authentic sample of **6a**, however, upon work-up we did not isolate any **6a**-hydrate.

In order to further validate our kinetic model (Fig. 7a and b), the microscopic rate constants (Fig. 7c) that we have measured by UV-vis spectrophotometry were inserted into the model and numerical methods were used to solve the

differential equations (Fig. 7b). The resulting predicted concentration-time profiles of all species were plotted (lines in Fig. 6c and d) to allow comparison with experimental data (dots in Fig. 6c and d).

Pleasingly, for the experiment performed in the absence of added water, the rapid evolution of **5a**-keto was modelled well by using ketonization and enolization rate constants (Table 1) for **4a** in MeCN. The addition of kinetic terms related to the auto-catalytic keto-enol tautomerism of **5a** were critical to the quantitative agreement between model and experiment for the formation of **6a**, with the formation of **6a** being predicted to reach only 1.7% after ~ 5 days in the absence of this contribution, but 2.9% (*versus* $\sim 4\%$ by experiment) when these terms were taken into account.

In the presence of 20% water, the build-up and break-down of **5a**-keto was modelled well alongside the profile for the formation of **6a**. We did not detect the presence of autocatalysis of the keto-enol equilibration of **5a** by our UV-vis kinetic studies, and thus did not include them in the model. However, at the higher concentrations employed in this NMR study, any

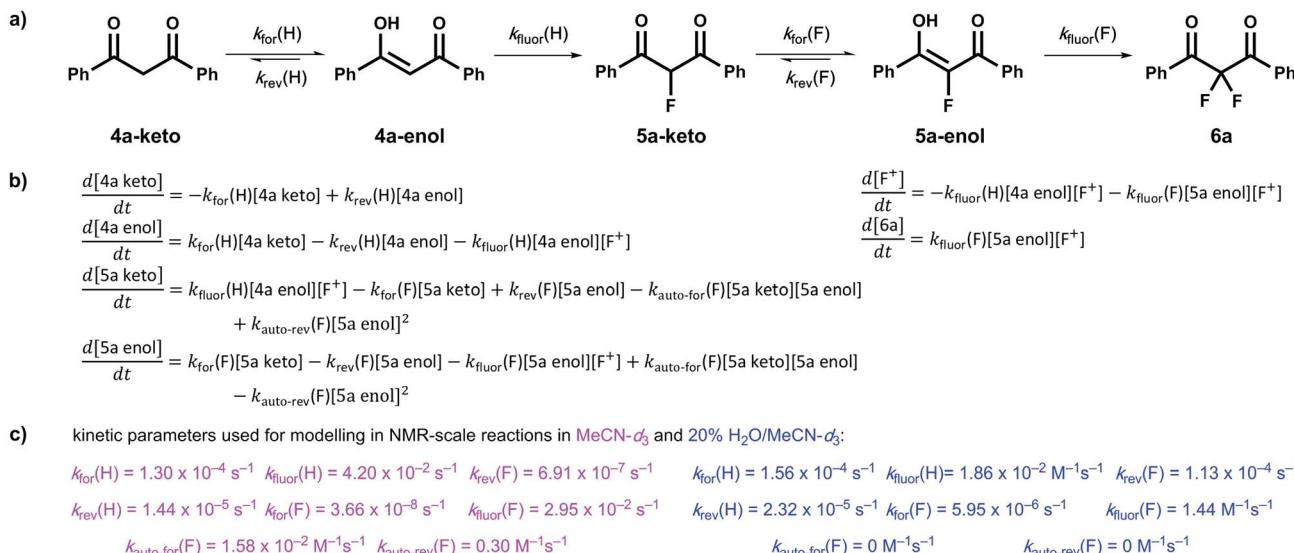


Fig. 7 (a) Overall kinetic model for the difluorination of compound **4a** with Selectfluor™. (b) Differential representations for the rates of formation of each species within the kinetic model, where $[F^+]$ represents the concentration of Selectfluor™. (c) Rate constants used for kinetic fitting of fluorination processes in $\text{MeCN}-d_3$ (pink) and in 20% water in $\text{MeCN}-d_3$ (blue). Values for $k_{\text{for}}(\text{H})$ and $k_{\text{rev}}(\text{H})$ were based on those observed in the presence of 240 mM $^7\text{Bu}_4\text{NBF}_4$, where these values were chosen to mimic the effect of salt. When a similar approach was adopted for $k_{\text{for}}(\text{F})$ and $k_{\text{rev}}(\text{F})$, poor fitting was observed. We attribute this to the extreme sensitivity of the tautomerization processes of the fluoro-system **5a**, described by these parameters, to the presence of small amounts of water that arise from the highly hygroscopic nature of the tetrabutylammonium salt.

such terms could become more sizeable and could contribute to improving the model.

3. Conclusions

We have utilized a photo-switching method for the determination of the effects of additives on keto-enol tautomerism in the 1,3-diaryl-1,3-dicarbonyls **4a-d** and the corresponding fluorinated derivatives **5a-d**. We have shown through kinetics studies that the addition of water is a simple method for increasing the rate of enolization and thus increasing the rate of formation of 2,2-difluoro-1,3-dicarbonyl **6a**. We found that small quantities of formic acid and DABCO greatly increased the enolization rate of **4a** and formic acid also increased the enolization rate of **5a**. The presence of DABCO resulted in the de-fluorination of **5a**, as evidenced by NMR studies, whereas **5b** was not de-fluorinated by DABCO. The non-fluorinated product of Selectfluor™, $\text{ClCH}_2\text{DABCO}^+\text{BF}_4^-$, which is rarely considered in synthetic application, had small but detectable effects on keto-enol equilibration kinetics, however, the nature of the effects is not clear.

We also obtained kinetic data on the fluorination of mono-fluoroenols **5a-d** with Selectfluor™ 1 and NFSI 2 under a variety of conditions. We have shown that the addition of a second fluorine atom occurs at a rate greater than or similar to that of the addition of the first fluorine atom. The rate-limiting step in the overall difluorination mechanism is therefore the enolization of the mono-fluoroketo tautomer, represented by $k_{\text{for}}(\text{F})$ in Fig. 7a.

Our kinetics studies correlate very well with previous synthetic studies; Banks *et al.*¹⁹ first reported the selective

monofluorination of **4a** using Selectfluor™ in MeCN, which gave 100% crude and 84% pure yields. We also observed complete conversion of **4a** to **5a** by both spectrophotometric and NMR methods, due to the high enol content of **4a**. Yi and co-workers^{64,65} reacted a series of aromatic 1,3-dicarbonyl compounds with 2.1 equivalents of Selectfluor™ in 10 : 1 MeCN/H₂O at 25 °C for 1–2 days, to obtain a range of 2,2-difluoro-1,3-diketones in approx. 90% yield. This matches our conclusion that water must be present to facilitate the enolization of **5a-keto** and thus allow difluorination to occur within reasonable timescales. Pattison *et al.*⁶⁶ attempted the difluorination of an aromatic β-ketoester with Selectfluor™ (2.5 equivalents) under reflux conditions in MeCN, which gave an 8 : 1 ratio of mono- and difluorinated products. This was attributed to the lower enol content of β-ketoesters compared to **4a**.⁶⁶ Since water was not used in the reaction, the enolization of the β-ketoester was presumably slow, which explains the low conversion to the difluorinated product. Stavber *et al.*²⁸ reported monofluorinations of cyclic 1,3-diketones and β-ketoesters in water using Selectfluor™ (1.1 equivalents), obtaining yields of 74–91%. The difluorinations of acyclic 1,3-diketones and β-ketoesters *via* Selectfluor™ (2.2 equivalents) in water gave yields of 78–89%. All reactions were conducted at 70 °C for 4–10 h. Fluorination of the acyclic 1,3-dicarbonyls could not be selectively stopped at the monofluorination stage, but by using 2.2 equivalents of Selectfluor™ the 2,2-difluoro-1,3-dicarbonyls were obtained without additional activation of the starting material. Syntheses of α,α -difluoro-β-ketoamides have been achieved using H₂O:PEG-400 solvent mixtures in the presence of K₂CO₃,⁶⁷ as well as very recently reported H₂O:MeCN

systems⁶⁸ in green chemistry research programs, for which our experiments provide supporting mechanistic evidence of the crucial roles of water and base.

Our studies give direct evidence that water plays an essential role in accelerating the enolization of mono-fluorodiketone derivatives to allow the formation of difluorodiketones. Our findings have important implications for synthetic fluorination procedures: the addition of small quantities of water to partially enolic 1,3-dicarbonyl derivatives increases rates of keto to enol tautomerism, supporting the formation of the key enol intermediates required for both the first and second fluorination steps. Furthermore, water also enhances the rate of fluorination of fluoroenols, again supporting the expedited formation of pharmaceutically relevant α,α -difluoroketonic compounds.

4. Methods

The ESI contains details of methods, kinetics experiments and product analyses.

Conflicts of interest

The authors declare no conflict of interest.

Acknowledgements

We are grateful to AstraZeneca and Durham University Science Faculty for providing doctoral funding to N. R. D. R. W. H thanks D. Jardine and M. Miller for their recommendation of numerical fitting software.

References

- 1 D. O'Hagan, *Chem. Soc. Rev.*, 2008, **37**, 308–319.
- 2 S. Purser, P. R. Moore, S. Swallow and V. Gouverneur, *Chem. Soc. Rev.*, 2008, **37**, 320–330.
- 3 K. Muller, C. Faeh and F. Diederich, *Science*, 2007, **317**, 1881–1886.
- 4 T. Liang, C. N. Neumann and T. Ritter, *Angew. Chem., Int. Ed.*, 2013, **52**, 8214–8264.
- 5 E. A. Ilardi, E. Vitaku and J. T. Njardarson, *J. Med. Chem.*, 2014, **57**, 2832–2842.
- 6 A. Harsanyi and G. Sandford, *Org. Process Res. Dev.*, 2014, **18**, 981–992.
- 7 M. Butters, J. Ebbs, S. P. Green, J. MacRae, M. C. Morland, C. W. Murtiashaw and A. J. Pettman, *Org. Process Res. Dev.*, 2001, **5**, 28–36.
- 8 B. L. Shapiro and M. M. Chrysam, *J. Org. Chem.*, 1973, **38**, 880–893.
- 9 W. J. Middleton and E. M. Bingham, *J. Am. Chem. Soc.*, 1980, **102**, 4845–4846.
- 10 B. Zajc and M. Zupan, *J. Chem. Soc., Chem. Commun.*, 1980, 759.
- 11 B. Zajc and M. Zupan, *J. Org. Chem.*, 1982, **47**, 573–575.
- 12 E. H. Appelman, L. J. Basile and R. C. Thompson, *J. Am. Chem. Soc.*, 1979, **101**, 3384–3385.
- 13 R. D. Chambers, M. P. Greenhall and J. Hutchinson, *J. Chem. Soc., Chem. Commun.*, 1995, 21–22.
- 14 R. D. Chambers, M. P. Greenhall and J. Hutchinson, *Tetrahedron*, 1996, **52**, 1–8.
- 15 R. D. Chambers and J. Hutchinson, *J. Fluorine Chem.*, 1998, **92**, 45–52.
- 16 R. D. Chambers, D. Holling, R. C. H. Spink and G. Sandford, *Lab Chip*, 2001, **1**, 132.
- 17 R. D. Chambers, M. A. Fox and G. Sandford, *Lab Chip*, 2005, **5**, 1132.
- 18 C. B. McPake and G. Sandford, *Org. Process Res. Dev.*, 2012, **16**, 844–851.
- 19 R. E. Banks, N. J. Lawrence and A. L. Popplewell, *J. Chem. Soc., Chem. Commun.*, 1994, 343–344.
- 20 J.-C. Xiao and J. M. Shreeve, *J. Fluorine Chem.*, 2005, **126**, 473–476.
- 21 L. Hintermann and A. Togni, *Angew. Chem., Int. Ed.*, 2000, **39**, 4359–4362.
- 22 S. Piana, I. Devillers, A. Togni and U. Rothlisberger, *Angew. Chem., Int. Ed.*, 2002, **41**, 979–982.
- 23 M. Althaus, C. Becker, A. Togni and A. Mezzetti, *Organometallics*, 2007, **26**, 5902–5911.
- 24 G. Stavber, M. Zupan and S. Stavber, *Tetrahedron Lett.*, 2007, **48**, 2671–2673.
- 25 J. L. Howard, Y. Sagatov and D. L. Browne, *Tetrahedron*, 2018, **74**, 3118–3123.
- 26 A. S. Reddy and K. K. Laali, *Tetrahedron Lett.*, 2015, **56**, 5495–5499.
- 27 G. Stavber, M. Zupan, M. Jereb and S. Stavber, *Org. Lett.*, 2004, **6**, 4973–4976.
- 28 G. Stavber and S. Stavber, *Adv. Synth. Catal.*, 2010, **352**, 2838–2846.
- 29 D. E. Yerien, S. Barata-Vallejo and A. Postigo, *Chem.-Eur. J.*, 2017, **23**, 14676–14701.
- 30 W. R. Dolbier, *Guide to Fluorine NMR for Organic Chemists*, John Wiley and Sons Inc., 2nd edn, 2016.
- 31 W. Peng and J. M. Shreeve, *J. Org. Chem.*, 2005, **70**, 5760–5763.
- 32 G. Pattison, *Eur. J. Org. Chem.*, 2018, **2018**, 3520–3540.
- 33 M. H. Gelb, J. P. Svaren and R. H. Abeles, *Biochemistry*, 1985, **24**, 1813–1817.
- 34 J. T. Welch and S. Eswarakrishnan, *Fluorine in Bioorganic Chemistry*, John Wiley and Sons, New York, 1991.
- 35 D. Schirlin, S. Baltzer, V. Van Dorsselaer, F. Weber, C. Weill, J. M. Altenburger, B. Neises, G. Flynn, J. M. Rémy and C. Tarnus, *Bioorg. Med. Chem. Lett.*, 1993, **3**, 253–258.
- 36 S. Giovani, M. Penzo, S. Brogi, M. Brindisi, S. Gemma, E. Novellino, L. Savini, M. J. Blackman, G. Campiani and S. Butini, *Bioorg. Med. Chem. Lett.*, 2014, **24**, 3582–3586.
- 37 N. Rozatian, I. W. Ashworth, G. Sandford and D. R. W. Hodgson, *Chem. Sci.*, 2018, **9**, 8692–8702.
- 38 D. S. Timofeeva, A. R. Ofial and H. Mayr, *J. Am. Chem. Soc.*, 2018, **140**, 11474–11486.
- 39 S. Wood, S. Etridge, A. Kennedy, J. Percy and D. J. Nelson, *Chem.-Eur. J.*, 2019, **25**, 5574–5585.
- 40 R. A. Morton, A. Hassan and T. C. Calloway, *J. Chem. Soc.*, 1934, 883–901.

41 P. Markov, *Chem. Soc. Rev.*, 1984, **13**, 69–96.

42 P. Markov and E. Radeva, *J. Photochem.*, 1975, **4**, 179–183.

43 P. Markov and I. Petkov, *Tetrahedron*, 1977, **33**, 1013–1015.

44 D. Veierov, T. Bercovici, Y. Mazur and E. Fischer, *J. Org. Chem.*, 1978, **43**, 2006–2010.

45 D. Veierov, T. Bercovici, E. Fisher, Y. Mazur and A. Yoge, *J. Am. Chem. Soc.*, 1973, **95**, 8173–8175.

46 D. Veierov, T. Bercovici, E. Fischer, Y. Mazur and A. Yoge, *J. Am. Chem. Soc.*, 1977, **99**, 2723–2729.

47 K. Sato, G. Sandford, K. Shimizu, S. Akiyama, M. J. Lancashire, D. S. Yufit, A. Tarui, M. Omote, I. Kumadaki, S. Harusawa and A. Ando, *Tetrahedron*, 2016, **72**, 1690–1698.

48 R. M. Claramunt, C. López, M. D. Santa María, D. Sanz and J. Elguero, *Prog. Nucl. Magn. Reson. Spectrosc.*, 2006, **49**, 169–206.

49 M. T. Rogers and J. L. Burdett, *Can. J. Chem.*, 1965, **43**, 1516–1526.

50 I. Andrae, A. Bringhen, F. Böhm, H. Gonzenbach, T. Hill, L. Mulroy and T. G. Truscott, *J. Photochem. Photobiol. B*, 1997, **37**, 147–150.

51 A. Cantrell and D. J. McGarvey, *J. Photochem. Photobiol. B*, 2001, **64**, 117–122.

52 J. F. Coetzee and G. R. Padmanabhan, *J. Am. Chem. Soc.*, 1965, **87**, 5005–5010.

53 B. G. Cox, *Acids and Bases: Solvent Effects on Acid-Base Strength*, Oxford University Press, 2013.

54 W. N. Olmstead and F. G. Bordwell, *J. Org. Chem.*, 1980, **45**, 3299–3305.

55 A. Kütt, I. Leito, I. Kaljurand, L. Sooväli, V. M. Vlasov, L. M. Yagupolskii and I. A. Koppel, *J. Org. Chem.*, 2006, **71**, 2829–2838.

56 A. Kundu, S. Pathak, K. Debnath and A. Pramanik, *Tetrahedron Lett.*, 2014, **55**, 3960–3968.

57 S. Pathak, A. Kundu and A. Pramanik, *RSC Adv.*, 2014, **4**, 10180–10187.

58 W. R. Dolbier, G. D. Purvis III, M. J. Seabury, G. E. Wicks and C. R. Burkholder, *Tetrahedron*, 1990, **46**, 7991–8004.

59 W. R. Dolbier, X. X. Rong and Y.-H. He, *Tetrahedron Lett.*, 1993, **34**, 5185–5188.

60 W. R. Dolbier and X. X. Rong, *Tetrahedron Lett.*, 1996, **37**, 5321–5324.

61 L. A. Kaplan and H. B. Pickard, *J. Chem. Soc. D*, 1969, 1500–1501.

62 Z. Zhang, Á. Puente, F. Wang, M. Rahm, Y. Mei, H. Mayr and G. K. S. Prakash, *Angew. Chem., Int. Ed.*, 2016, **55**, 12845–12849.

63 R. McMullan and G. A. Jeffrey, *J. Chem. Phys.*, 1959, **31**, 1231–1234.

64 J. Qian, W. Yi, X. Huang, J. P. Jasinski and W. Zhang, *Adv. Synth. Catal.*, 2016, **358**, 2811–2816.

65 Y. Lin, W. Yi, W. Shen and G. Lu, *Org. Lett.*, 2016, **18**, 592–595.

66 D. J. Leng, C. M. Black and G. Pattison, *Org. Biomol. Chem.*, 2016, **14**, 1531–1535.

67 Z. Zhang, J. Bi, Q. Liu and G. Zhang, *J. Fluorine Chem.*, 2013, **151**, 45–49.

68 L. Tang, Z. Yang, J. Jiao, Y. Cui, G.-D. Zou, Q. Zhou, Y.-Q. Zhou, W.-H. Rao and X. Ma, *J. Org. Chem.*, 2019, **84**, 10449–10458.